FINITE ELEMENT ANALYSIS OF FATIGUE CRACK GROWTH THRESHOLD TESTING TECHNIQUES

S. R. Daniewicz and J. D. Skinner

Department of Mechanical Engineering
Mississippi State University
Mississippi State, Mississippi, USA

ABSTRACT

Three-dimensional elastic-plastic finite element analyses were conducted to model fatigue crack growth in an M(T) specimen. Variable amplitude loading with a continual load reduction was used to simulate the load history associated with fatigue crack growth threshold measurement. Load reductions with both constant load ratio R and constant maximum stress intensity K_{max} were used.

Results indicated that load reduction with constant R generated a plastic wake such that remote crack opening occurred during loading, with the crack front opening prior to a region remote to the crack front. The last region to open was located at the point at which the load reduction originally began, and at the free surface. For the limited amount of crack growth simulated, this crack opening was observed to occur when the applied stress level was approximately 70% of the maximum stress. Remote crack opening and large opening stresses have previously been associated with large fatigue crack growth threshold measurements.

INTRODUCTION

Measurement of the fatigue crack growth threshold ΔK_{th} for large cracks requires that a gradual reduction in the stress intensity factor range be applied during a fatigue crack growth test. The ASTM standard test method E647 recommends that the load ratio R be held fixed during the required load reduction. In an attempt to avoid plasticity-induced crack closure as the threshold is approached, an alternative load reduction has been proposed in which the maximum stress intensity factor K_{max} is held constant. This type of load reduction results in a continually increasing R such that threshold measurement is made in the absence of crack closure. The resulting effective threshold stress intensity $(\Delta K_{eff})_{th}$ is often referred to as an intrinsic measurement of fatigue crack growth resistance [1,2,3,4]. However, Donald and Paris [5] have suggested a K_{max} effect such that both $(\Delta K_{eff})_{th}$ and K_{max} are needed to define resistance to fatigue crack growth in the threshold regime.

When a load reduction using a fixed R is used, plasticity-induced closure will occur and the presence of the plastic wake can influence the resulting measured threshold. The effective and applied stress intensity factor ranges ΔK_{eff} and ΔK are related as follows

$$\frac{\Delta K_{eff}}{\Delta K} = \frac{S_{max} - S_o}{S_{max} - S_{min}} = \frac{1 - S_o / S_{max}}{1 - R} \tag{1}$$

where S_{max} and S_o are the maximum and opening stresses respectively. From Eqn. 1, the relationship between ΔK_{th} and $(\Delta K_{eff})_{th}$ may be written as

$$\Delta K_{th} = \frac{1-R}{1-S_o/S_{max}}\left(\Delta K_{eff}\right)_{th} \tag{2}$$

If one considers $(\Delta K_{eff})_{th}$ to be a material constant, then changes in the crack opening stress S_o will result in changes in the measured threshold ΔK_{th}. The measured threshold is now a function of plasticity-induced closure and no longer an intrinsic measurement of fatigue crack growth resistance. Eqn. 2 is applicable to threshold tests with fixed R load reduction only, since under a fixed K_{max} load reduction there is no closure in the threshold regime with $S_o/S_{max} \rightarrow R$ and $\Delta K_{th} = (\Delta K_{eff})_{th}$.

Donald and Paris [5] conducted fatigue crack growth experiments using 6061-T6 and 2024-T3 aluminum alloy M(T) specimens, and measured opening loads using compliance measurements. In the threshold regime, they conducted load shedding at fixed load ratios of R = 0.1 and 0.7. The data generated at R = 0.7 was a closure-free baseline data set with $\Delta K = \Delta K_{eff}$. Donald and Paris demonstrated that above the threshold regime, the closure-free data and the data generated at R = 0.1 correlated well when the measured opening loads were used to compute ΔK_{eff}. In the threshold regime, however, the measured opening stresses became excessively large such that the subsequently computed $(\Delta K_{eff})_{th}$ were too small when compared with the baseline data. These observations can be explained with the aid of Eqn. 2.

Two-dimensional analyses conducted by Newman [6] using a modified strip-yield model indicated that under load reduction with a fixed load ratio R, remote crack closure away from the crack tip can occur. This remote crack closure results in the crack tip opening prior to regions remote to the crack tip during loading, and a subsequent rapid rise in the magnitude of the opening stress S_o required to open the crack. These large opening stress values would in turn lead to large ΔK_{th} values (or alternatively small $(\Delta K_{eff})_{th}$ values) as seen from Eqn. 2. Newman showed that this remote closure occurs within the region in which constant amplitude pre-cracking was terminated and the load shedding procedure was initiated. It should be noted that Newman did not observe remote closure and elevated crack opening stresses when using lower stress levels. Analyses conducted using a load reduction with a fixed K_{max} resulted in closure-free crack surfaces as the threshold was approached, with the opening load below the minimum load.

Two-dimensional plane stress analyses were also conducted by McClung [7,8], using both the finite element method [7,8] and a modified strip-yield model [8]. The type of load reduction considered was restricted to fixed R. McClung observed elevated crack opening stresses from the finite element analyses during the load reduction, although these elevated opening stresses were not associated with remote closure except for simulations employing large initial stress intensity factor ranges ΔK_o.

The objective of this paper is to numerically model fatigue crack growth in a middle-crack tension M(T) specimen undergoing cyclic loading with a load reduction to confirm the existence of remote closure. Three-dimensional elastic-plastic finite element analyses were used to model the plasticity-induced closure developed, and the subsequent crack opening behavior, under a gradually reducing stress intensity factor range. Load reduction schemes under both constant R and constant K_{max} were also compared.

The two-dimensional modified strip-yield model analyses conducted by Newman averaged three-dimensional constraint effects through the thickness using an empirical constraint factor. The analyses conducted by McClung considered only plane stress. The three-dimensional analyses conducted in this study allowed a more realistic three-dimensional perspective of the plastic wake and subsequent crack opening behavior. However, while Newman and McClung utilized many analyses to investigate the effects of numerous variables, the current study was limited to two finite element analyses.

FINITE ELEMENT MODELING METHODOLOGIES AND DIFFICULTIES

The use of three-dimensional elastic-plastic finite element analysis to model plasticity-induced closure in cracked bodies undergoing cyclic loading has been limited as discussed by McClung [9]. Chermahini et al. [10,11] used three-dimensional elastic-plastic analyses to investigate the crack opening behavior of M(T) specimens under constant amplitude loading. Chermahini et al. [12] and Zhang et al. [13] performed similar analyses focused on the more complex semi-elliptical surface crack under constant amplitude loading.

Utilizing three-dimensional finite element analyses to model plasticity-induced closure is in general a computationally intensive effort because the finite element models required have a large number of elements and must be analyzed multiple times in succession. A large number of elements is necessary to insure adequate mesh refinement so that perhaps 5-10 elements exist within the plastic zone at any point on the crack front under the maximum loading. Alternately, mesh refinement requirements may be defined using the reversed plastic zone generated upon unloading [9]. To adequately model through-thickness effects, a relatively large number of elements are required through the specimen thickness as well.

Crack growth under cyclic loading is then simulated by loading the model with the maximum stress level of interest, and then releasing the nodes along the crack front to increase the crack size by one element. The applied stress is then reduced to the minimum stress of interest, thus completing one load cycle which corresponds to a crack tip advancement *da* equal to one element size. Each load cycle then corresponds to two monotonic analyses. For constant amplitude loading, perhaps 5 load cycles are required to achieve an approximate steady state condition in which the crack opening loads remain relatively constant.

The computationally intensive nature of three-dimensional plasticity-induced closure simulation is further aggravated when a variable amplitude load reduction such as that used for threshold measurement is considered as was done in the current study. Large amounts of crack growth are required to generate meaningful results in which the stress intensity factor range undergoes a significant reduction. To simulate large amounts of crack growth under the cyclic loading, a large number of load cycles are required which will generally exceed the number needed for a constant amplitude simulation. In addition, the decreasing maximum stress intensity associated with fixed R load shedding results in a decreasing plastic zone size along the crack front. This necessitates a more refined mesh to insure an adequate number of elements in the plastic zone as the maximum stress intensity factor diminishes. To the author's knowledge, three-dimensional finite element analyses using load reduction to simulate the load histories associated with threshold measurement have not been previously undertaken.

FINITE ELEMENT ANALYSES

The M(T) specimen exhibits three planes of symmetry, and consequently only one eighth of the geometry was modeled using eight-noded hexahedral elements as illustrated in Figure 1. The model consisted of a total of 13,430 nodes and 12,906 elements. Both model generation and solution were performed using the commercial finite element analysis program ANSYS 5.4. A thickness B = 4.78 mm, width W = 80 mm, and crack length $2a$ = 34 mm were used. The material was assumed to be an elastic-perfectly plastic aluminum alloy with modulus E = 70.0 GPa and flow stress σ_o = 400 MPa. The von Mises yield criterion and the associated flow rule were used. Small deformation theory was employed. A total of 25 load cycles were used for the load reduction with fixed R, while a total of 19 load cycles were used for the load reduction with fixed K_{max}. The crack front was advanced one element size during each cycle with da = 0.125 mm. With 25 load cycles, the fixed R load reduction analysis corresponded to 50 monotonic analyses conducted sequentially, an enormous computational burden given the size of the model employed.

To advance the crack, node release at the maximum applied load was performed in an incremental manner to avoid convergence difficulties [14]. This was accomplished using bundles of truss elements to initially connect all nodes which were later to be released as part of the analysis. These truss elements were then released individually such that total node release took place in an incremental manner. Contact elements were placed along the crack surface, allowing the contact stress along the crack surface to be computed.

This enabled a determination of the opening load as that load which first produced zero contact stress along the entire crack surface during loading. The contact elements also allowed a determination of which region of the crack surface was the last to open under an increasing load.

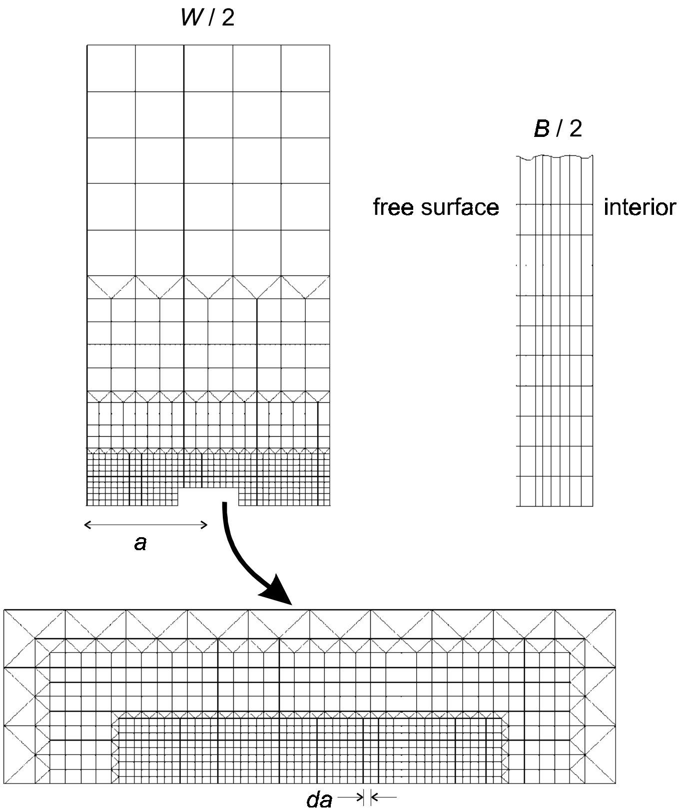

Figure 1: M(T) finite element model

Due to the computationally intensive nature of the analyses, the number of finite element analyses conducted was limited to two. The first modeled a load reduction conducted under fixed R conditions, while the second considered load reduction with a constant K_{max}. The load shedding used was defined using the following relationship

$$\Delta K = \Delta K_o e^{C\Delta a} \quad (3)$$

where Δa is the amount of crack growth following pre-cracking, ΔK_o is the initial stress intensity factor range at the start of load reduction, and C is a constant. In the current study, ΔK_o = 30 MPa√m was used. For the loading with fixed R, a value of R = 0 was used. For the loading with fixed K_{max}, a value of K_{max} = 30 MPa√m was used. Of the total load cycles employed, 5 were used to simulate constant amplitude pre-cracking with $\Delta K = \Delta K_o$ and R = 0. The remaining load cycles were used to simulate load shedding such that Δa = 2.5 mm for the fixed R load reduction and Δa = 1.75 mm for the load reduction with fixed K_{max}.

While ASTM E647 recommends a maximum value for C of – 0.08/mm, a value of –0.25/mm was employed in this study. This large value was chosen because small values of C result in the need for large amounts of crack growth before appreciable reductions in the stress intensity factor range are produced. Large amounts of crack growth in turn require an excessive number of sequential finite element analyses.

With the Δa as given above and C = –0.25/mm, the final ΔK employed during the load shedding was 16.1 MPa√m for the fixed R load reduction and 19.4 MPa√m for the load reduction with fixed K_{max} as computed using Eqn. 3. It should be noted that these values are well above the threshold value for aluminum alloys. Consequently, while the simulations performed addressed the load shedding process used for threshold measurement, they did not consider the threshold regime directly.

To validate the adequacy of the mesh refinement used, a monotonic analysis was performed using an applied stress intensity of K = 30 MPa√m. In the crack plane ahead of the crack front, the plastic zone size varied and was found to encompass between 9 and 13 elements. This level of refinement was considered adequate. Assuming the crack tip plastic zone is proportional to K^2, for K = 16 MPa√m the plastic zone would encompass between 3 and 4 elements. At this level of stress intensity, which would exist at the termination of the fixed R load reduction, the level of refinement is suspect.

The total amount of crack growth modeled considering both the pre-cracking and the load shedding was δa = 3.125 mm (fixed R) and 2.375 mm (fixed K_{max}). The newly formed crack surface formed by the crack growth is illustrated in Figure 2 for the fixed R load reduction. Following the simulation of crack growth, the contact stress on the rectangular region shown was monitored using contact elements to determine which region was the last to open under an increasing applied stress.

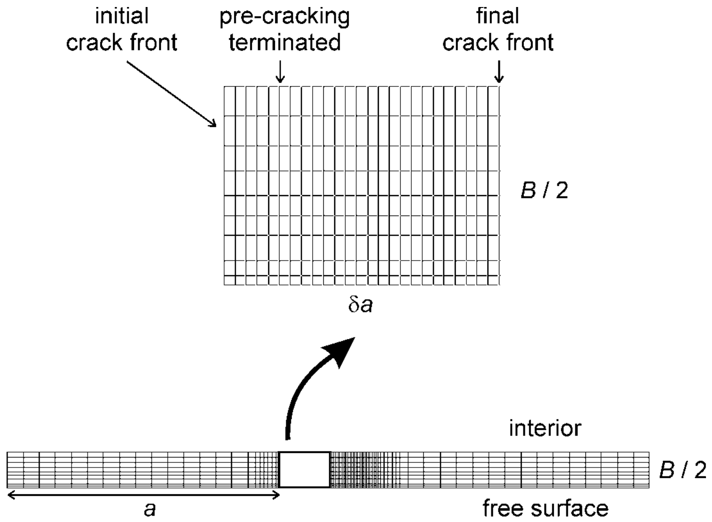

Figure 2: Crack surface formed by cyclic loading (fixed R load reduction)

Results for the crack growth simulations with fixed R and fixed K_{max} are shown respectively in Figures 3 and 4. The dark areas indicates regions of the crack surface which are closed. From Figure 3, note that remote closure was observed such that the crack front was not the last region to open. The crack front region was observed to open at an applied stress of $S/S_{max} \approx$ 0.40, while the crack became completely open at a value of $S/S_{max} \approx$ 0.70. The last region to open was located at the free surface where the pre-cracking was terminated.

The observed normalized opening stress value $S_o/S_{max} \approx 0.70$ is a relatively large value. Constant amplitude three-dimensional finite element analyses conducted by Chermahini et al. [10] at an applied stress level of S_{max}/σ_o = 0.25 resulted in $S_o/S_{max} \approx 0.60$. No remote closure was observed, with the crack front at the free surface being the last region to open. This lower opening stress value was generated at a higher applied stress level than was used for the load shedding. In general, for constant amplitude loading, increases in the applied stress result in lower opening stresses. Thus, it is unclear whether the increased opening stress value determined from the fixed R load shed was due to remote closure or simply the result of a lower applied stress (the analysis started with $S_{max}/\sigma_o \approx 0.29$ and terminated with $S_{max}/\sigma_o \approx 0.12$). It should also be noted that an increase in the amount of simulated crack growth for the fixed R load reduction analysis could result in an increased opening stress, with the normalized opening stress possibly exceeding the value of 0.70 determined here.

From Figure 4, for a load reduction with a fixed maximum stress intensity factor, the crack front was the last region to open and remote closure was not observed. Again, the last region to open was located at the free surface. The opening stress for this load reduction was similar to that determined for the fixed R load reduction with $S/S_{max} \approx 0.72$. Thus, while the crack opening behaviors for fixed R and fixed K_{max} were significantly different, the magnitude of the opening stresses were essentially the same. Clearly, the amount of crack growth simulated was not sufficiently large to produce a closure free condition, which is the intent during threshold measurement. The results shown in Figure 4 suggest that the threshold regime is approached without the occurrence of remote closure.

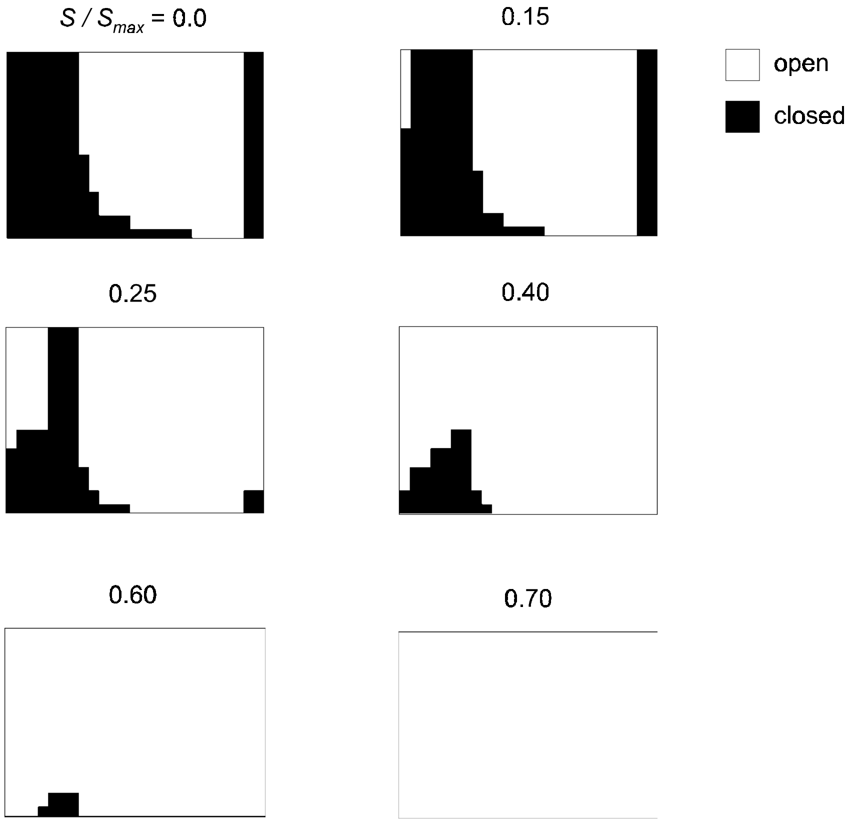

Figure 3: Crack opening behavior under fixed load ratio

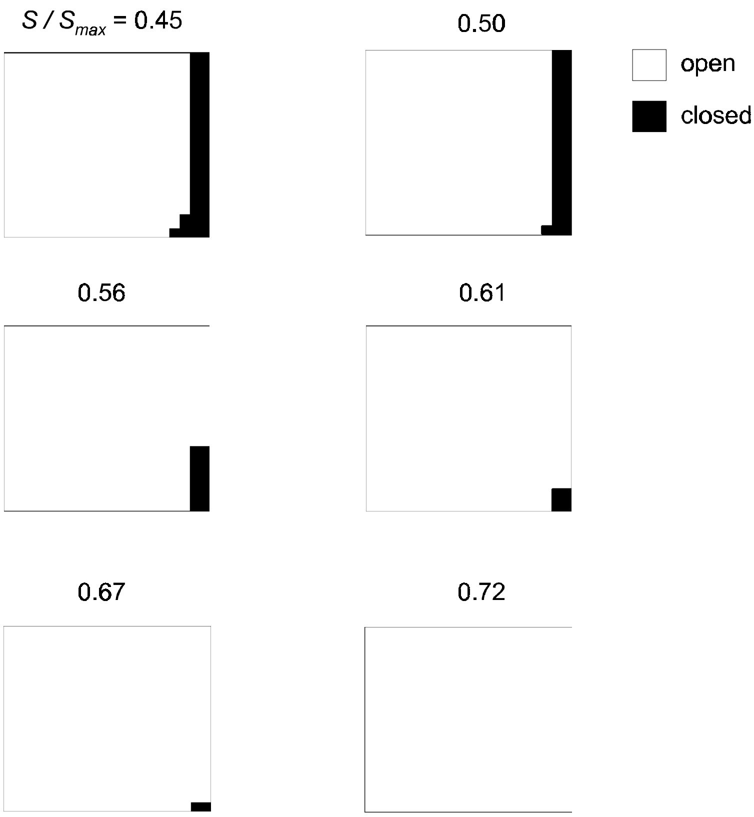

Figure 4: Crack opening behavior under fixed maximum stress intensity

SUMMARY AND CONCLUSIONS

Three-dimensional elastic-plastic finite element analyses were conducted to model fatigue crack growth in an M(T) specimen. Variable amplitude loading with a continual load reduction was used to simulate the load history associated with fatigue crack growth threshold measurement. The analyses were conducted to confirm the existence of remote closure, in which the crack front opens prior to a region remote to the crack front.

Results indicated the crack opening process is three-dimensional in nature, with regions in the interior opening prior to regions near the free surface. Load reduction with constant R generated a plastic wake such that remote crack opening occurred during loading. The last region to open was located at the point at which the load reduction originally began, and at the free surface. This remote opening resulted in an opening stress S_o with $S_o/S_{max} \approx 0.70$. In contrast, for load reduction with constant K_{max}, the crack front was the last to open with a similar opening stress of $S_o/S_{max} \approx 0.72$. The amount of crack growth simulated for the load reduction with constant K_{max} was not sufficiently large to produce a closure free condition, which is the intent of such a test.

Due to the severe computational requirements of simulating fatigue crack growth and plasticity-induced closure in three-dimensional bodies undergoing large amounts of crack growth, only two analyses were performed. The results given are thus limited in scope and further research is required to assess the effects of the initial stress intensity factor range ΔK_o, the load ratio R, the load shed rate constant C, and material properties such as flow stress and strain hardening. The amount of crack growth modeled was also limited, such that the final ΔK values used were not in the threshold regime. Further research is needed using models which simulate more extensive crack growth to explore the crack opening behavior in the threshold regime.

REFERENCES

1. Doker, H., Bachmann, V., and Marci, G. (1982). In: *Fatigue Thresholds*, p. 45, EMAS, Warley.
2. Herman, W. A., Hertzberg, R. W., Newton, C. H., and Jaccard, R. (1987). In: *Fatigue '87, Third International Conference on Fatigue and Fatigue Thresholds*, Vol. II, pp. 819-828.
3. Marci, G., Castro, D. E., and Bachmann, V. (1989) *J. Test Eval.*, **17**, 28.
4. Hertzberg, R. W. (1995) *Material Science & Engineering*, **A190**, 25.
5. Donald, J. K. and Paris, P. C. (1998) In: Proceedings of *Fatigue Damage of Structural Materials* II.
6. Newman, J. C. (1999). In: *Fatigue Crack Growth Thresholds, Endurance Limits, and Design, ASTM STP 1372*, American Society for Testing and Materials.
7. McClung, R. C. (1991) *International Journal of Fracture* **52**, 145.
8. McClung, R. C. (1999). In: *Fatigue Crack Growth Thresholds, Endurance Limits, and Design, ASTM STP 1372*, American Society for Testing and Materials.
9. McClung, R. C. (1999) In: *Fatigue '99, Seventh International Fatigue Conference.*
10. Chermahini, R. G., Shivakumar, K. N., and Newman, J. C. (1988). In: *Mechanics of Fatigue Crack Closure, ASTM STP 982*, American Society for Testing and Materials, pp. 398-413.
11. Chermahini, R. G. and Blom A. F. (1991) *Theoretical and Applied Fracture Mechanics* **15**, 267.
12. Chermahini, R. G., Palmberg, B., and Blom, A. F. (1993) *Int. J. of Fatigue* **15**, 259.
13. Zhang, J. Z. and Bowen, P. (1998) *Engineering Fracture Mechanics* **60**, 341.
14. Wu, J. and Ellyin, F. (1996) *International Journal of Fracture* **82**, 43.